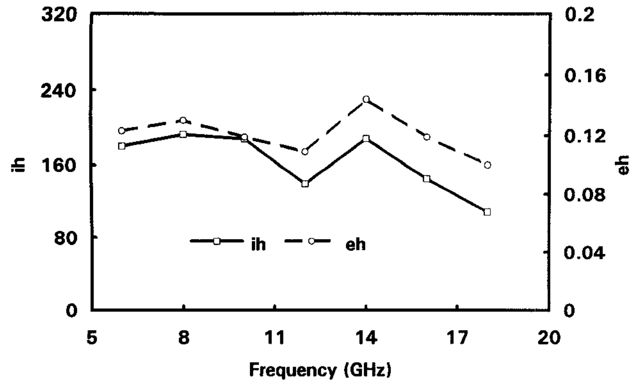

Fig. 8. The strength of a noise current source in $(pA)^2$/Hz and a noise voltage source in $(nV)^2$/Hz as extracted from measured data in H-parameter format. Parasitic elements and Cdg and Rgs shown in Fig. 5 have been de-embedded.

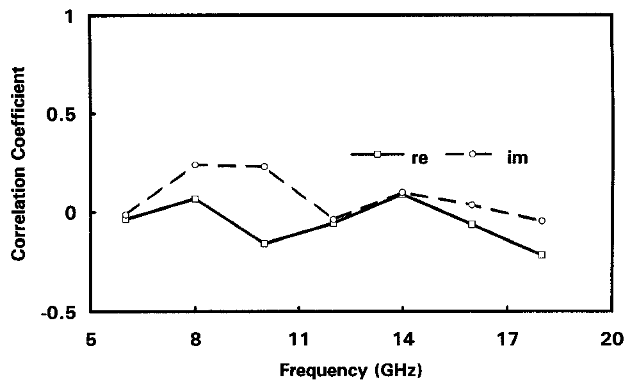

Fig. 9. The correlation coefficient between the noise current source and the noise voltage source shown in Fig. 8 as extracted from measured data.

in Figs. 3 and 4. Quite good agreement is observed. Several other HEMTs have been analyzed and modeled with similar results.

V. Conclusions

A procedure for noise source extraction from measured data was presented. Experimental data from a low-noise HEMT device showed little correlation between input and output noise when the noise sources were extracted in H-parameter format forcing open-circuit conditions at the gate and short-circuit conditions at the drain. The experimental data show that an accurate HEMT noise model may be constructed using non-correlated noise sources.

Acknowledgment

The author wishes to thank Dr. Paul Saunier for device fabrication and Mr. Mark A. Walker for noise parameter measurements.

References

[1] H. A. Haus (Chairman), "Representation of noise in linear two-ports," *Proc IRE*, vol. 48, pp. 69–74, Jan. 1960.
[2] H. Rothe and W. Dahlke, "Theory of noisy fourpoles," *Proc. IRE*, vol. 44, pp. 811–818, June 1956.
[3] A. Riddle, "Extraction of FET model noise-parameters from measurement," in *1991 IEEE MTT-S Int. Microwave Symp. Dig.*, pp. 1113–1116.
[4] Circuit simulator software available from EEsof, Inc., Westlake Village, CA 91362.
[5] G. Dambrini *et al.*, "A new method for determining the FET small-signal equivalent circuit," *IEEE Microwave Theory Tech.*, vol. 36, no. 7, pp. 1151–1159, July 1988.
[6] R. A. Pucel, H. A. Haus, and H. Statz, "Signal and noise properties of gallium arsenide microwave field-effect transistors," in *Advances in Electronics and Electron Physics*, vol. 38, L. Morton, Ed., New York: Academic Press, 1975.
[7] M. W. Pospieszalski, "Modeling of noise parameters of MESFET's and MODFET's and their frequency and temperature dependence," *IEEE Trans Microwave Theory Tech.*, vol. 37, pp. 1340–1350, Sept. 1989.

An Efficient Method for the Determination of Resonant Frequencies of Shielded Circular Disk and Ring Resonators

Faton Tefiku and Eikichi Yamashita

Abstract— **This short paper describes an efficient method for the determination of resonant frequencies of shielded circular disks and annular ring resonators. Bounary integral equations are set up based on the Green's identity in the circular cylindrical coordinates, and are numerically solved by discretizing common boundary integral paths. The overall integration path is considerably shortened to reduce computation time by using simple eigen functions satisfying regular homogeneous boundary conditions as weighting functions instead of using Green's functions. Computational results for both circular disks and annular rings are presented and compared with other available numerical results for some cases. This method can be extended to treat thick conductors.**

I. Introduction

Circular disks and annular ring conductors printed on a dielectric substrate are finding a wide range of applications in microwave integrated circuits. Various simple models have been employed in the past to estimate the resonant frequencies of these structures: a simple cavity model with magnetic side walls [1], [2], a modified cavity model [3], a planar waveguide model [4] [5] taking into account fringe fields for both circular disk and annular ring resonators. A more rigorous method was developed for an annular ring using the reaction concept [6]. With a full wave analysis in the Hankel transform domain it was possible to estimate both resonant frequencies and radiation patterns [7], [8]. Calculations have also been made under the assumption of a conductive shielding in the case of resonator structures with high dielectric permittivities or thin substrates [9], [10].

The boundary integral equation method without using Green's function has been proposed [11] and has recently been employed in the analysis of planar transmission lines [12]. It is one of the features of the method that eigen functions satisfying the regular boundary conditions of the shielding conductor are used instead of Green's function. The manipulation with complicated Green's functions is avoided in this way and the overall integration path is considerably shortened for saving the computational time.

In this short paper, we develop the above boundary integral equation method in the circular cylindrical coordinates to solve

Manuscript received March 16, 1992; revised May 26, 1992.
The authors are with the Department of Electronic Engineering, University of Electro-Communications, Chofugaoka 1-5-1, Chofu-Shi, Tokyo 182, Japan.
IEEE Log Number 9204494.

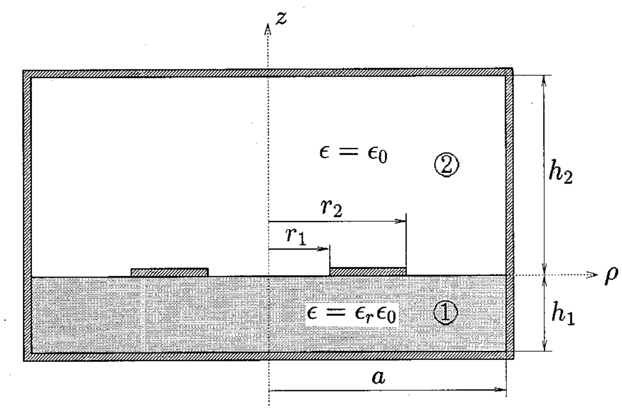

Fig. 1. Cross-section of a circular resonator structure.

subject problems. Resonant frequencies for various dimensions of circular disks and annular rings are calculated and compared with presently available data.

II. Boundary Integral Equation Method

The structure to be analyzed consists of a circular ring resonator printed on a dielectric substrate enclosed in a cylindrical metallic box whose cross-section and dimensions are shown in Fig. 1. A hybrid-mode analysis is necessary for this inhomogeneous structure which is divided into two homogeneous subregions.

In formulating the boundary integral equation, the z components of the electromagnetic fields are chosen as unknown wave functions satisfying the Helmholtz equations. Simple eigen functions satisfying the same wave equation are selected as weighting functions. Then, the following equations can be derived from the Green's identity for the axial components, E_z and H_z, in each homogeneous region:

$$\oint_\Gamma \left(E_z \frac{\partial \Psi^e}{\partial n} - \Psi^e \frac{\partial E_z}{\partial n} \right) \rho \, d\Gamma = 0 \tag{1a}$$

$$\oint_\Gamma \left(H_z \frac{\partial \Psi^h}{\partial n} - \Psi^h \frac{\partial H_z}{\partial n} \right) \rho \, d\Gamma = 0 \tag{1b}$$

where Ψ^e and Ψ^h denote the eigen function of the E type and H type, respectively, and the azimuthal dependence of the electromagnetic field is assumed as $e^{jn\phi}$.

Eigen functions, Ψ^e and Ψ^h, as the general solutions of the wave equation in the circular cylindrical coordinates in each homogeneous region are obtained by the method of the separation of variables. After applying the boundary conditions on the surface of the metallic box to the general solution, the eigen functions for the subregion 1 and subregion 2 are expressed as

$$\Psi_1^e = J_n(\alpha_m \rho) \cos [k_{z1e}(z + h_1)] \tag{2a}$$

$$\Psi_1^h = J_n(\beta_m \rho) \sin [k_{z1h}(z + h_1)] \tag{2b}$$

$$\Psi_2^e = J_n(\alpha_m \rho) \cos [k_{z2e}(z - h_2)] \tag{2c}$$

$$\Psi_2^h = J_n(\beta_m \rho) \sin [k_{z2h}(z - h_2)] \tag{2d}$$

where the factor $e^{jn\phi}$ has been omitted and α_m and β_m are the solutions of the equations:

$$J_n(\alpha_m \rho)|_{\rho=a} = 0 \qquad (m = 1, 2, \cdots) \tag{3a}$$

and

$$\left. \frac{\partial J_n(\beta_m \rho)}{\partial \rho} \right|_{\rho=a} = 0 \qquad (m = 1, 2, \cdots) \tag{3b}$$

where $k_{z1e}, k_{z1h}, k_{z2e}$, and k_{z2h} are given as

$$\begin{aligned} k_{z1e} &= \sqrt{\varepsilon_r k_0^2 - \alpha_m^2} \qquad & k_{z1h} &= \sqrt{\varepsilon_r k_0^2 - \beta_m^2} \\ k_{z2e} &= \sqrt{k_0^2 - \alpha_m^2} \qquad & k_{z2h} &= \sqrt{k_0^2 - \beta_m^2} \end{aligned} \tag{4}$$

and k_0 is the wave number for free space and J_n is the nth order Bessel function of the first kind.

By substituting the above eigen functions into (1), four boundary integral equations can be constructed. Then, the axial components of electromagnetic fields are expressed in term of fields tangential to the interface using Maxwell's equations. The continuity condition of tangential electromagnetic fields is applied to the air-dielectric interface and the resonator conductor is assumed to have zero thickness. After some manipulations with the E type and H type equations, a set of two integral equations can be derived as fellows:

$$\begin{aligned} A_{nm} &\int_{\Gamma_d} \left\{ \frac{1}{\rho} \frac{\partial}{\partial \rho}(\rho E_\rho) - \frac{n}{\rho} E_\phi \right\} J_n(\alpha_m \rho) \rho \, d\rho \\ &+ B_{nm} \int_{\Gamma_c} \left\{ -\frac{1}{\rho} \frac{\partial}{\partial \rho}(\rho I_\rho) + \frac{n}{\rho} I_\phi \right\} J_n(\alpha_m \rho) \rho \, d\rho = 0 \end{aligned} \tag{5a}$$

$$\begin{aligned} C_{nm} &\int_{\Gamma_d} \left\{ -\frac{n}{\rho} E_\rho + \frac{1}{\rho} \frac{\partial}{\partial \rho}(\rho E_\phi) \right\} J_n(\beta_m \rho) \rho \, d\rho \\ &+ D_{nm} \int_{\Gamma_c} \left\{ \frac{n}{\rho} I_\rho - \frac{1}{\rho} \frac{\partial}{\partial \rho}(\rho I_\phi) \right\} J_n(\beta_m \rho) \rho \, d\rho = 0 \end{aligned} \tag{5b}$$

where E_ρ and E_ϕ are the tangential components of the electric field on the air-dielectric interface, and $I_\rho = H_{\phi 1} - H_{\phi 2}$ and $I_\phi = H_{\rho 2} - H_{\rho 1}$ are the two components of the surface current density on the circular resonator. Γ_d denotes the air-dielectric interface and Γ_c the conductor surface of the resonator in the cross section. The boundary integrals on the conductor enclosure part disappear because of the nature of the eigen functions satisfying the boundary conditions. The factors, A_{nm}, B_{nm}, C_{nm} and D_{nm}, are defined as

$$\begin{aligned} A_{nm} &= \varepsilon_r \cos (k_{z1e} h_1) k_{z2e} \sin (k_{z2e} h_2) \\ &\quad + \cos (k_{z2e} h_2) k_{z1e} \sin (k_{z1e} h_1) \end{aligned} \tag{6a}$$

$$B_{nm} = k_{z1e} \sin (k_{z1e} h_1) k_{z2e} \sin (k_{z2e} h_2) \tag{6b}$$

$$\begin{aligned} C_{nm} &= k_{z1h} \cos (k_{z1h} h_1) \sin (k_{z2h} h_2) \\ &\quad + k_{z2h} \cos (k_{z2h} h_2) \sin (k_{z1h} h_1) \end{aligned} \tag{6c}$$

$$D_{nm} = k_0^2 \sin (k_{z1e} h_1) \sin (k_{z2e} h_2) \tag{6d}$$

For numerical processing, the above boundary integral paths are divided into M $(M = N_d + N_c)$ finite segments, where N_d and N_c denote the number of segments on the Γ_d and Γ_c path, respectively. The components of the electric field and the current density are considered as unknown constants at each segment of the discretized boundary integral paths. When the number of the eigen functions is selected to be equal to the number of divided segments, M, a set of homogeneous linear equations can be obtained from (5), in a matrix form as

$$\begin{bmatrix} [a^e] & [b^e] & [c^e] & [d^e] \\ [a^h] & [b^h] & [c^h] & [d^h] \end{bmatrix} \begin{bmatrix} [E_\rho] \\ [E_\phi] \\ [I_\rho] \\ [I_\phi] \end{bmatrix} = [0] \tag{7}$$

The coefficients of the sub-matrices are given as a product of the factors in (6) and the solutions of one of the integrals below

$$H_1(\gamma_i, \rho_j) = \int_{\rho_{j-1}}^{\rho_j} \frac{n}{\rho} J_n(\gamma_k \rho_j) \rho \, d\rho \tag{8a}$$

$$H_2(\gamma_i, \rho_j) = H_1(\gamma_i, \rho_j) - \int_{\rho_{j-1}}^{\rho_j} \gamma_i \rho J_{n-1}(\gamma_i \rho_j) \, d\rho \tag{8b}$$

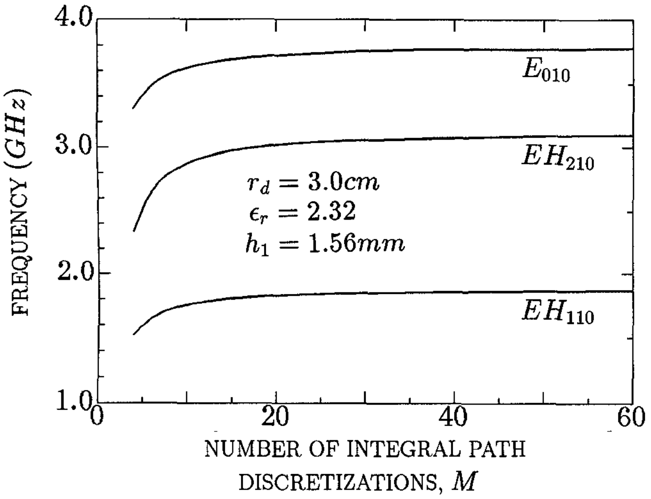

Fig. 2. Convergence of first three resonant frequencies for a circular disk resonator against the number of integral path discretization, $M, (h_2 = 15h_1, a = 6.0$ cm).

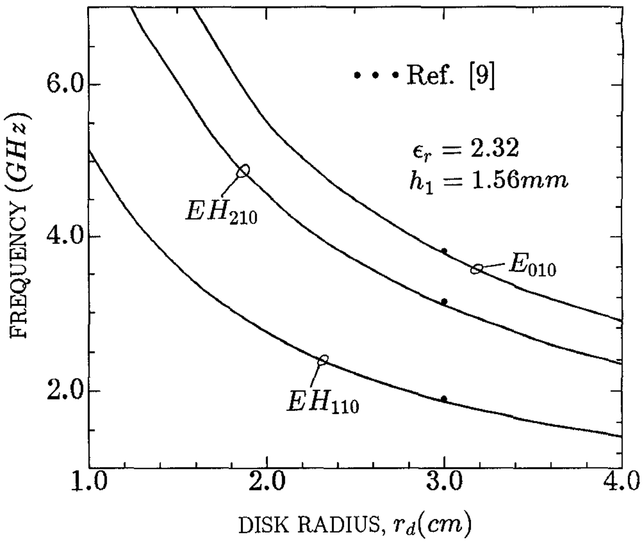

Fig. 3. Resonant frequencies of a circular disk resonator ($h_2 = 15h_1, a = 3 \sim 7$ cm).

where $\rho_j - \rho_{j-1}$ is the width of the jth segment and γ_i takes values α_i or β_i, for the E type or H type equations, respectively.

Non-trivial solutions of (7) exist if its determinant vanishes. Then, k_0 corresponding to the resonant frequencies of the structure can be determined.

III. Numerical Results

In general, the zeros of the determinant of (7) represent resonant frequencies of the whole structure, that is, the shielded circular resonator. However, the proper choice of dimensions of shielding walls results in solutions close to those of an open resonator structure, or distorted fields of the modes of a partially dielectric filled cylindrical cavity. We follow the same rule as one given in [10], where the dimensions of the shielding walls were chosen so as to produce no strong mutual coupling between cavity modes and disk and ring modes for the same order, n. In other words, the effect of the shielding walls can be neglected if h_2 and a are large enough and the above resonance positions are avoided.

The resonant frequencies of the partially dielectric filled cylindrical cavity can be easily calculated as shown below. Removing the circular conductor from the interface, the second part of (5) disappears. The procedure to find cavity mode resonances is simplified as one to find zeros of the following equations:

$$A_{nm} = 0 \tag{9a}$$

$$C_{nm} = 0 \tag{9b}$$

The solutions of (9a) and (9b) are used to predict the resonance frequencies of the distorted fields of the modes of the partially dielectric filled cylindrical cavity and to determine proper dimensions of the shielding walls.

Fig. 2 shows the convergence properties of resonant frequencies for the dominant mode and two higher order modes of a circular disk against the total number of segments, M. The dimensions of the disk resonator are $r_1 = 0, r_2 = r_d = 3.0$ cm, $h_1 = 1.56$ mm, $\varepsilon_r = 2.32$, and those of the shielding walls are $h_2 = 15h_1, a = 6.0$ cm. It is found that taking $M = 40$ in total ensures computation errors of less than 0.5 percent. The typical computation time is about 20 seconds for one resonant frequency on a Sun 4 workstation, where about ten iterations are performed for convergence with a good first guess.

Fig. 3 shows the first three resonant frequencies of the circular disk as the function of the disk radius, r_d, with parameters of $\varepsilon_r = 2.32$ and $h_1 = 1.56$ mm. The shielding height is fixed as $h_2 = 15h_1$, and the shielding radius takes values of $a = 3 \sim 7$ cm in order to avoid the mutual coupling. The case $r_d = 3.0$ cm is the same as those studied in [9]. The difference less than 1 percent between our numerical results and those given in [9] is found for all the three modes.

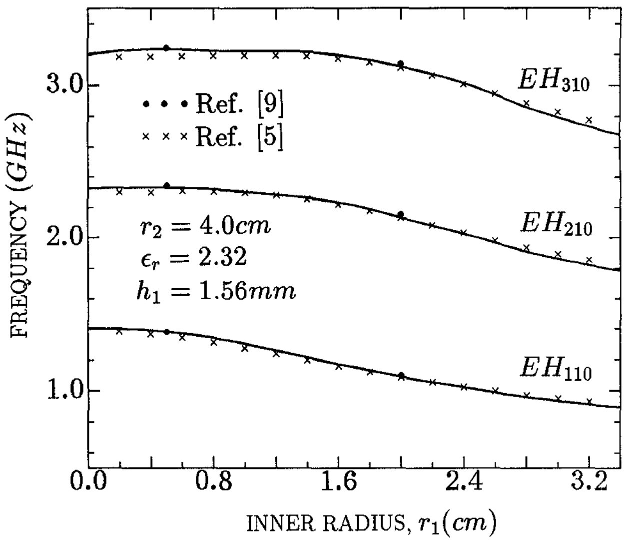

Fig. 4. Resonant frequencies of a circular ring resonator ($h_2 = 15h_1, a = 7.0$ cm).

The resonant frequencies of circular rings were also investigated. Fig. 4 shows the first three resonant frequencies of a circular ring versus the inner radius, r_1, with parameters of $r_2 = 4.0$ cm, $\varepsilon_r = 2.32$ and $h_1 = 1.56$ mm. The dimensions of the shielding enclosure are $h_2 = 15h_1$ and $a = 7.0$ cm. Good agreement with the numerical result of [9] is found again for two particular cases, $r_1 = 0.5$ cm and $r_1 = 2.0$ cm. This fact seems to confirm the exactness of these two methods.

Some numerical computations were also performed for comparison with the planar waveguide model with frequency dependent effective parameters [5]. In general, good agreement was found as long as the circular conductor occupies a considerable portion of the integral path. However, when $w = r_2 - r_1$ is decreased, stray fields around the circular conductor are increased and the influence of the shielding is significant even without strong coupling between circular ring modes and cavity modes. These phenomena must be taken into account in the computation if a resonator has to be completely enclosed with a shielding housing.

For the case of open structures, better approximations can be achieved using thin substrates and high dielectric permittivities.

ACKNOWLEDGMENT

The authors wish to thank Professor K. Atsuki, Dr. N. Kishi and Mr. H. Kirino, Research Student, of the University of Electro-communications for their helpful comments, discussions and technical support.

REFERENCES

[1] S. Mao, S. Jones and G. D. Vendelin, "Millimeter-wave integrated circuits," *IEEE Trans Microwave Theory Tech.*, vol. 16, pp. 455–461, 1968.
[2] Y. S. Wu and F. J. Rosenbaum, "Mode chart for microstrip ring resonators," *IEEE Trans. Microwave Theory and Tech*, vol. 21, pp. 487–489, July 1973.
[3] I. Wolf and N. Knoppik, "Rectangular and circular microstrip disk capacitors and resonators," *IEEE Trans. Microwave Theory Tech.*, vol. 22, pp. 857–864, Oct. 1974.
[4] R. P. Ovens, "Curvature effects in microstrip ring resonators," *Electron. Lett.*, vol. 12, pp. 356–357, July 1976.
[5] A. M. Khilla, "Computer-aided design for microstrip ring resonators," in *Proc. 11th European Microwave Conf.*, Amsterdam, 1981, pp. 1–6.
[6] S. G. Pintzos and R. Pregla, "A simple method for computing the resonant frequencies of microstrip ring resonators," *IEEE Trans. Microwave Theory Tech.*, vol. 26, pp. 809–813, Oct. 1978.
[7] K. Araki and T. Itoh, "Hankel transform domain analysis of open circular microstrip radiating structures," *IEEE Trans. Antennas Propagat.*, vol. 29, pp. 84–89, Jan. 1981.
[8] S. M. Ali, W. C. Chew, and J. A. Kong, "Vector Hankel transform analysis of annular-ring microstrip antenna," *IEEE Trans. Antennas Propagat*, vol. 30, pp. 637–644, July 1982.
[9] R. Jansen, "Computer analysis of shielded microstrip structures," *AEU 29*," pp. 241–247, 1975.
[10] R. Jansen, "High-order finite element polynomials in the computer analysis of arbitrary shaped microstrip resonators," *AEÜ 30*, pp. 71–79, 1976.
[11] N. Kishi and T. Okoshi, "Proposal for a boundary-integral method without using Green's function," *IEEE Trans. Microwave Theory Tech.*, vol. 35, pp. 887–892, Oct. 1987.
[12] L. Zhu and E. Yamashita, "New method for the analysis of dispersion characteristics of various planar transmission lines with finite metallization thickness," *IEEE Microwave Guided Wave Lett.*, vol. 1, pp. 164–166, July 1991.

Design Analysis of Novel Coupling Structures for Multilayer MMIC's

Matthew Gillick, Ian D. Robertson, and Jai S. Joshi

***Abstract*—Novel monolithic multilayered coupling structures are presented and their performances analyzed. These structures have reduced current crowding at their conductor edges compared to coplanar type coupling structures, and are particularly suitable for integration with multi-dielectric MMIC's. This paper presents the closed-form analytical expressions for the coupler's even and odd mode impedances and coupling coefficients derived using conformal mapping techniques. These direct formulas have the advantage of being well suited for the computer aided design analysis of MMIC's without the need for lengthy numerical modelling techniques.**

I. INTRODUCTION

Multilayer MMIC's have recently been receiving widespread attention [1]–[3]. Various small size novel coupling structures incorporating multi-dielectric layers have been proposed and analyzed [4]–[7]. This paper presents a new multilayer homogeneous coupling structure which offers reduced current crowding at the conductor edges, and is particularly suitable for integration with coplanar waveguide, slot line, and microstrip transmission lines. By having the transmission lines perpendicular to the ground plane(s), as shown in Fig. 1, the level of current crowding at the conductor edges may be reduced compared to coplanar type structures [8]. This is evident since the electric field distribution across two conductor surfaces is more uniform for a given conductor spacing when they are perpendicular, than when they are within the same plane. The fabrication of these couplers could be realized using newly developed multilayer MMIC technologies. A combination of successive wet etching, reactive ion etching or plasma etching of multi-dielectric layers could be used to fabricate a channel-shaped cut out, whereby perpendicular strip conductors may be realized.

II. ANALYSIS OF THE COUPLING STRUCTURES

The proposed coupling structures are illustrated in Fig. 1, where $2h$ is the total substrate thickness, $2s$ is the spacing between the coupled lines, and $2w$ is the gap width in the center ground plane. Structure B, has two additional ground shieldings parallel to the center ground plane, placed at a distance $h - r$ from each conductor strip. Throughout these multilayer structures, the dielectric substrate has a constant relative permitivity, ε_r. Shown in Fig. 2, is an example of the variation between the even and odd-mode electric field lines of structure A.

The following quasi-static analysis employs a sequence of conformal mappings to evaluate the even and odd mode capacitances of the couplers. The analytical approach used here isolates the even and odd modes in order to evaluate their impedances and subsequently the structure's coupling factors. For both structures the metallic

Manuscript received April 21, 1992; revised June 1, 1992. This work was supported by the Science and Engineering Research Council (SERC) UK and by British Aerospace Space Systems Limited, UK.

M. Gillick and I. D. Robertson are with the Communications Research Group, Department of Electronic and Electrical Engineering, King's College, University of London, Strand, London, UK, WC2R 2LS.

J. S. Joshi is with the Satellite Payload Engineering Department, British Aerospace Space Systems Limited, Argyle Way, Stevenage, Herts, UK, SG1 2AS.

IEEE Log Number 9204495.